# Modified Faddeev treatment of electron capture

Steven Alston*
*Theoretical Physics, University of Tennessee, Knoxville, Tennessee 37996*
*and Physics Department, The Pennsylvania State University, Wilkes-Barre Campus, Lehman, Pennsylvania 18627*
(Received 21 December 1994; revised manuscript received 8 December 1995)

The Faddeev multiple-scattering formalism in second order is modified to treat lower projectile energies. The electronic part of the amplitude is evaluated using a Hartree-Fock approximation to the helium wave function and a consistent screened target potential for the active electron. Off-energy-shell scattering states appearing in the electronic part of the full amplitude are corrected for loss of normalization. The high velocity Faddeev nuclear-scattering contribution is normalized to the eikonally transformed electronic amplitude at large angles. An application to proton-helium collisions at 293 keV shows good agreement with the experimental data. The effects of the various approximations are studied.

PACS number(s): 34.70.+e

## I. INTRODUCTION

For incident energies of a few MeV, the second-order Faddeev treatment [1] of electron capture has been shown to reproduce well the experimental differential cross section in proton-helium and proton-hydrogen collisions [2]. At these energies, the contribution of multiple scatterings is significant because of the important role played by the Thomas mechanism [3]. The Faddeev scattering formalism breaks the full collision into two-body collisions, which are described by transition operators [4]. Like the second-order Born treatment, the Faddeev treatment maintains the simple double-scattering description of the Thomas mechanism while providing *quantitative* agreement with the experimental data [5], even at projectile scattering angles beyond 1 mrad, where nuclear scattering dominates.

In the present paper, a modified Faddeev formalism is applied to collisions at lower velocities which, however, are high enough for the perturbative approach to remain valid. At the lower velocities, the multiple-scattering treatment can still allow for the interaction of one scattering with another. Additionally, a more accurate representation of the ground-state wave function of helium may improve the cross section as a result of the redistribution of important bound-state momentum components. This question is addressed by comparing cross sections calculated using single- and double-$\zeta$ wave functions [6]. (The double-$\zeta$ wave function approximates the Hartree-Fock limit.) Consistent with the better wave function, a target potential is also employed which accounts for the screening of the target nucleus by the other electron. A comparison is made between the capture amplitude based on a two-body Coulomb target scattering amplitude with screened charge and a better one, which is the sum of a Coulomb amplitude (with the charge of the residual ion) and a short-range amplitude [7].

The Faddeev treatment describes the capture of the electron by means of wave packets of virtual off-the-energy-shell scattering states representing collisions with the projectile and target ions. Marxer and Briggs [8] have shown that these wave packets lose normalization as the velocity decreases. In a strong-potential approach, they developed a modified theory that corrects for the loss of normalization and shows good agreement with experiment. The Marxer-Briggs method is applied here to the wave packets used in the electron–target-core and electron–projectile-ion scatterings of the Faddeev formalism.

The internuclear-scattering contribution is included in the Faddeev formalism, but an accurate evaluation is difficult at lower velocities. It is nonetheless desirable to relate this contribution to a simple picture of Rutherford-like scattering with, however, the requisite off-shell corrections being included, even if the norm of the amplitude is not adequate. The internuclear contribution can also be determined by using the eikonal approach [9], a general application of which proceeds by transforming the electronic amplitude in the wave picture to impact-parameter space, multiplying the transformed amplitude by the eikonal phase factor $b^{2iZ_PZ_T/v}$, where $b$ is the impact parameter, $Z_P$, $Z_T$ are the projectile and target-nuclear charges, and $v$ is the impact velocity, and then transforming back to the wave picture. The eikonal factor is derived from the transverse components of the internuclear motion. At angles beyond 1 mrad, the Faddeev internuclear contribution can be normalized to the eikonal result, which is done in the present work.

An exact numerical evaluation of the rest of the amplitude is infeasible with the use of a screened target potential. The treatment presented here, which relies on the smallness of the binding energy of the electron relative to its scattering energy, employs near-the-energy-shell representations of the two-body transition matrices, and further, neglects factors of the order of $m/M_P$ and $m/M_T$ (with $m$, $M_P$, and $M_T$ being the electron, projectile, and target-nuclear masses) [1].

The above approach is applied to proton-helium collisions at an incident energy of 293 keV, corresponding to a velocity of 3.43 au. Calculated differential cross sections are compared with the experimental data [5] and with the results of a two-state atomic expansion (2SAE) [10] and the continuum distorted-wave (CDW) theory [11].

The plan of the paper is the following. The second-order Faddeev amplitude is specified in Sec. II, including both the

*Permanent address: Physics Department, The Pennsylvania State University, Wilkes-Barre Campus, Lehman, PA 18627.

 

electronic and internuclear parts. In Sec. III, the use of a better target wave function and potential, as well as the method for the normalization of the off-shell scattering states, are presented. Section IV compares calculated results with experiment and other theory and gives a comparative analysis of the effects of the various refinements. Atomic units are used.

## II. THE SECOND-ORDER FADDEEV AMPLITUDE FOR CAPTURE

### A. General setup

Within a one-electron model, a three-body collision is considered where a projectile ion $P$ is incident on a target consisting of an electron $e$ and a target ion $T$:

$$P+(T+e)\rightarrow(P+e)+T,$$

where parentheses denote bound electron-ion aggregates. Either the target or projectile may contain passive electrons. Accordingly, the two-body interactions between each pair of particles assume the general modified Coulomb form [12].

The Faddeev formalism, as applied to the electron-capture problem with particular emphasis on the points relevant to the present treatment and subsequent approximate evaluation, is outlined here. (A detailed discussion is given elsewhere [1].) Splitting the collision into two-body components, Faddeev defined the (channel) operators $\mathscr{T}_a$ $(a=Pe,Te,PT)$ that solve the matrix equation [4]

$$\begin{bmatrix}\mathscr{T}_{Te}\\ \mathscr{T}_{Pe}\\ \mathscr{T}_{PT}\end{bmatrix}=\begin{bmatrix}0\\ \tilde{\mathscr{T}}_{Pe}\\ \tilde{\mathscr{T}}_{PT}\end{bmatrix}+\begin{bmatrix}0 & \tilde{\mathscr{T}}_{Te} & \tilde{\mathscr{T}}_{Te}\\ \tilde{\mathscr{T}}_{Pe} & 0 & \tilde{\mathscr{T}}_{Pe}\\ \tilde{\mathscr{T}}_{PT} & \tilde{\mathscr{T}}_{PT} & 0\end{bmatrix}G_o^+\begin{bmatrix}\mathscr{T}_{Te}\\ \mathscr{T}_{Pe}\\ \mathscr{T}_{PT}\end{bmatrix}, \tag{1}$$

where the $\tilde{\mathscr{T}}_a$ denote transition matrices for the mutual scattering of two particles while the third one propagates freely and $G_o^+(E)$ is the free Green operator for total energy $E$. Zeros along the diagonal of the square matrix ensure that repeated multiple scatterings of the *same* two particles with free propagation of the third do not occur, which would otherwise lead to ill-defined amplitudes. Equation (1) is solved approximately by an iterative Neumann scheme in which the first-order solution is $\mathscr{T}_a^{(1)}=\tilde{\mathscr{T}}_a$ $(a=Pe,PT)$ and $\mathscr{T}_{Te}^{(1)}=0$, and the higher-order terms $\mathscr{T}_a^{(n)}$ $(n>1)$ are obtained by substituting $\mathscr{T}_a^{(n-1)}$ into the right-hand side of Eq. (1) and performing the matrix multiplication.

In terms of the $\mathscr{T}_a$, the transition operator for the capture (rearrangement, in general) process is given by

$$\mathscr{T}_C=V_{Pe}+\mathscr{T}_{Te}+\mathscr{T}_{PT}. \tag{2}$$

In the present work, a second-order approximation to the $\mathscr{T}_a$ is used to obtain $\mathscr{T}_C$. Following Eqs. (1) and (2), one finds

$$\begin{aligned}\mathscr{T}_C^{(2)}\approx&[V_{Pe}+\tilde{\mathscr{T}}_{Te}G_o^+(E)\tilde{\mathscr{T}}_{Pe}]\\ &+[\tilde{\mathscr{T}}_{PT}+\tilde{\mathscr{T}}_{PT}G_o^+(E)\tilde{\mathscr{T}}_{Pe}+\tilde{\mathscr{T}}_{Te}G_o^+(E)\tilde{\mathscr{T}}_{PT}]\\ \equiv&\mathscr{T}_e+\mathscr{T}_n.\end{aligned} \tag{3}$$

In the last part of Eq. (3), the various contributions have been collected into separate operators $\mathscr{T}_e$ and $\mathscr{T}_n$, which arise, respectively, from the direct transfer of the electron and the internuclear scattering.

The individual two-body potentials do not have simple coordinate dependences; however, they reduce asymptotically to

$$\begin{aligned}V_{Pe}(r_P)&\sim-Z_P^\infty/r_P \quad \text{as } r_P\rightarrow\infty,\\ V_{Te}(r_T)&\sim-Z_T^\infty/r_T \quad \text{as } r_T\rightarrow\infty,\\ V_{PT}(R)&\sim Z_P^\infty Z_T^\infty/R \quad \text{as } R\rightarrow\infty.\end{aligned} \tag{4}$$

The projectile and target nuclear charges in Eqs. (4) are $Z_P$ and $Z_T$ and the corresponding asymptotic charges are $Z_P^\infty$ and $Z_T^\infty$. The shielding of the projectile and target nuclei by the nonactive electrons leads to the values $Z_P^\infty$ and $Z_T^\infty$; for neutral targets $Z_T^\infty$ is unity.

Forming the matrix element of $\mathscr{T}_e+\mathscr{T}_n$ between initial and final asymptotic scattering states, the second-order Faddeev approximation (F2) to the exact capture amplitude, at energy $E$, is

$$A_{F2}(E)=\langle\Phi_f|\mathscr{T}_e+\mathscr{T}_n|\Phi_i\rangle\equiv A_e+A_n, \tag{5}$$

where the asymptotic states are given by

$$\begin{aligned}\langle\mathbf{R}_T,\mathbf{r}_T|\Phi_i\rangle&=e^{i\mathbf{K}_i\cdot\mathbf{R}_T}\phi_i(\mathbf{r}_T),\\ \langle\mathbf{R}_P,\mathbf{r}_P|\Phi_f\rangle&=e^{i\mathbf{K}_f\cdot\mathbf{R}_P}\phi_f(\mathbf{r}_P).\end{aligned} \tag{6}$$

In Eq. (6), the initial and final bound states are $\phi_i$ and $\phi_f$, and $\mathbf{K}_i$ and $\mathbf{K}_f$ are the initial and final heavy-particle wave vectors. The coordinates of the electron relative to the projectile and target ions are denoted by $\mathbf{r}_P$ and $\mathbf{r}_T$, respectively; the projectile coordinates relative to the target ion, by $\mathbf{R}$, the projectile-electron system coordinates relative to the target ion, by $\mathbf{R}_P$, the projectile coordinates relative the target, by $\mathbf{R}_T$, and the electron coordinates relative the projectile-ion–target-ion center of mass, by $\mathbf{r}$ [13].

The free Green operator is

$$G_o^+(E)=(E-H_o+i\eta)^{-1}, \tag{7}$$

where the free Hamiltonian takes the possible forms

$$\begin{aligned}H_o&=-\frac{1}{2\nu_f}\nabla_{\mathbf{R}_P}^2-\frac{1}{2\mu_f}\nabla_{\mathbf{r}_P}^2\\ &=-\frac{1}{2\nu_i}\nabla_{\mathbf{R}_T}^2-\frac{1}{2\mu_i}\nabla_{\mathbf{r}_T}^2\\ &=-\frac{1}{2\nu_n}\nabla_{\mathbf{r}}^2-\frac{1}{2\mu_n}\nabla_{\mathbf{R}}^2.\end{aligned}$$

The total collision energy is given by $E=(1/2\nu_i)K_i^2+\varepsilon_i=(1/2\nu_f)K_f^2+\varepsilon_f$, where $\varepsilon_i$ and $\varepsilon_f$ are the initial and final bound-state energies. Initial, final, and internuclear internal and relative reduced masses and associated mass ratios for the two-body combinations are defined as $\mu_i=mM_T/(m+M_T)$, $\nu_i=M_P(m+M_T)/(m+M_P+M_T)$,

$\alpha=M_T/(m+M_T)$, $\mu_f=mM_P/(m+M_P)$, $\nu_f=M_T(m+M_P)/(m+M_P+M_T)$, $\beta=M_P/(m+M_P)$, $\mu_n=M_PM_T/(M_P+M_T)$, $\nu_n=m(M_T+M_P)/(m+M_P+M_T)$, $\gamma=M_T/(M_P+M_T)$. Initial and final heavy-particle velocities are defined in terms of the initial and final wave vectors as $\mathbf{v}_i=\mathbf{K}_i/\nu_i$ and $\mathbf{v}_f=\mathbf{K}_f/\nu_f$. One can show that $v_f/v_i=1+O(m/M_P)+O(m/M_T)$ and, for forward-angle capture, that $\mathbf{v}_f\cdot\mathbf{v}_i=1+O(m/M_P)+O(m/M_T)$; thus, the projectile velocity is written as $\mathbf{v}$.

If the transition matrices $\tilde{\mathscr{T}}_a$ in the second-order terms in Eq. (3) are approximated to first order by potentials $V_a$ and the first-order term $\tilde{\mathscr{T}}_{PT}$ is approximated to second order by $V_{PT}+V_{PT}G_o^+(E)V_{PT}$, one obtains the second-order Born operator [14]

$$\mathscr{T}_{B2}^{(2)}=V_{Pe}+V_{Te}G_o^+(E)V_{Pe}+V_{PT}+V_{PT}G_o^+(E)V_{PT}+V_{PT}G_o^+(E)V_{Pe}+V_{Te}G_o^+(E)V_{PT}. \tag{8}$$

The internuclear terms of Eq. (8) can be shown to give no contribution to the cross section at forward scattering angles. The amplitude derived from the electronic part is compared with the Faddeev approximation below.

For each of the two-body collisions in the amplitude, it is useful to integrate the third free-particle motion so that two-body transition matrices can be obtained. Later, these transition matrices will be approximated by forms near the energy shell.

### B. Reduction of the electronic term to two-body *T*-matrix form

In the electronic part of the amplitude Eq. (5), the double-scattering term is separated, giving

$$A_e=\langle\Phi_f|V_{Pe}|\Phi_i\rangle+\langle\Phi_f|\tilde{\mathscr{T}}_{Te}G_o^+(E)\tilde{\mathscr{T}}_{Pe}|\Phi_i\rangle \equiv A_{B1}+A_e^{(2)}, \tag{9}$$

where $A_{B1}$ is the first Born amplitude. The first Born amplitude [15] takes the form

$$A_{B1}=-4\pi^3(K^2+Z_P^2)\tilde{\phi}_f(\mathbf{K})^*\tilde{\phi}_i(-\mathbf{J}) \tag{10}$$

for $i=f=1s$. The $1s$ hydrogenic wave function in momentum space is $\tilde{\phi}_{1s}(\mathbf{k})=(2^3Z^5)^{1/2}/\pi(k^2+Z^2)^2$. The partial amplitude Eq. (10) becomes large as $v\to Z_T$, since $J\to Z_P$, and this behavior provides the dominant feature of the cross section. The momentum transfers that are experienced by the target ion and projectile during the collision have been defined as

$$\mathbf{J}=\alpha\mathbf{K}_i-\mathbf{K}_f, \quad \mathbf{K}=\beta\mathbf{K}_f-\mathbf{K}_i. \tag{11}$$

The components parallel to $\mathbf{v}$ are $K_z=-v/2+(\varepsilon_i-\varepsilon_f)/v$ and $J_z=-v/2+(\varepsilon_f-\varepsilon_i)/v$, and the components perpendicular to it are $K_\perp$ for $\mathbf{K}$ and $-K_\perp$ for $\mathbf{J}$. Momentum conservation for the process takes the form $\mathbf{K}+\mathbf{J}+\mathbf{v}=\mathbf{0}$.

In the second-order term in Eq. (9), the operation of $G_o^+$ and $\tilde{\mathscr{T}}_{Pe}$ to the right on the $\mathbf{R}_P$ plane wave and of $\tilde{\mathscr{T}}_{Te}$ to the left on the $\mathbf{R}_T$ plane wave, together with Fourier analyses of the bound-state wave functions and insertion of complete sets of plane-wave states in $\mathbf{r}_P$ and $\mathbf{R}_P$ between $\tilde{\mathscr{T}}_{Te}$ and $G_o^+$, lead to the expression

$$A_e^{(2)}=(2\pi)^{-3}\int d\mathbf{k}_f d\mathbf{k}_i\tilde{\phi}_f(\mathbf{k}_f)^*\tilde{\phi}_i(\mathbf{k}_i) \times T_{Te}(\mathbf{k}_f+\mathbf{v},\mathbf{k}_i+\mathbf{k}_f-\mathbf{K};E_f)\tilde{G}_o^+(E_i) \times T_{Pe}(\mathbf{k}_f+\mathbf{k}_i+\mathbf{J},\mathbf{k}_i-\mathbf{v};E_i) \tag{12}$$

for the partial amplitude. The $\delta$ functions arising from the heavy-particle integrations have been used to evaluate the momentum integrals of the complete sets. With terms of order $m/M_P$ and $m/M_T$ neglected, the scattering energies

$$E_i\approx\tfrac{1}{2}v^2-\mathbf{v}\cdot\mathbf{k}_i+\varepsilon_i, \quad E_f\approx\tfrac{1}{2}v^2+\mathbf{v}\cdot\mathbf{k}_f+\varepsilon_f \tag{13}$$

are obtained.

The two-body transition matrix is defined as

$$T(\mathbf{k}',\mathbf{k};\varepsilon)\equiv\left\langle\mathbf{k}'\left|V\left[1+\left\{\varepsilon+\frac{1}{2\mu}\nabla_{\mathbf{r}}^2-V+i\eta\right\}^{-1}V\right]\right|\mathbf{k}\right\rangle \equiv\langle\mathbf{k}'|V|\psi_{\varepsilon,\mathbf{k}}^+\rangle \tag{14}$$

for a potential $V$. Equation (14) defines the off-energy-shell scattering state $\psi_{\varepsilon,\mathbf{k}}^+$ of energy $\varepsilon$ and momentum $\mathbf{k}$, satisfying outgoing-wave boundary conditions. The transition matrices $T_{Pe}$ and $T_{Te}$ in Eq. (12) are derived, respectively, from the potentials $V_{Pe}$ and $V_{Te}$; they are completely off the energy shell: $k^2\neq2\mu\varepsilon$ and $k'^2\neq2\mu\varepsilon$, with $\mu$ denoting $\mu_i$ for $T_{Te}$ or $\mu_f$ for $T_{Pe}$.

The Fourier transform of the free Green function Eq. (7) appearing in Eq. (12) can assume either of two equivalent forms:

$$\tilde{G}_o^+(E_i)=[E_i-\tfrac{1}{2}(\mathbf{k}_i+\mathbf{k}_f+\mathbf{J})^2+i\eta]^{-1} =[E_f-\tfrac{1}{2}(\mathbf{k}_i+\mathbf{k}_f-\mathbf{K})^2+i\eta]^{-1}, \tag{15}$$

which will be useful later.

Equation (12) represents an electronic ''wave packet'' of momentum distribution $\phi_i(\mathbf{k}_i)$ centered about $-\mathbf{v}$ scattering in the projectile frame. The energy of each component is $E_i(\mathbf{k}_i)$. In the collision of the wave packet with the projectile, each component undergoes a momentum transfer $\mathbf{k}_f-\mathbf{K}$, as described by the transition matrix $T_{Pe}$. After propagating freely (represented by $\tilde{G}_o^+$), the packet, as seen now from the target frame, scatters off the target ion with each component undergoing a momentum transfer $-\mathbf{k}_i-\mathbf{J}$, as described by the transition matrix $T_{Te}$. The final momentum distribution centered on $\mathbf{v}$ is $\phi_f(\mathbf{k}_f)$, with energy $E_f(\mathbf{k}_f)$ for each component.

### C. Reduction of the internuclear term to two-body $T$-matrix form

The partial amplitude

$$A_n=\langle\Phi_f|\widetilde{\mathscr{T}}_{PT}|\Phi_i\rangle+\langle\Phi_f|\widetilde{\mathscr{T}}_{Te}G_o^+(E)\widetilde{\mathscr{T}}_{PT}|\Phi_i\rangle+\langle\Phi_f|\widetilde{\mathscr{T}}_{PT}G_o^+(E)\widetilde{\mathscr{T}}_{Pe}|\Phi_i\rangle\equiv A_n^{(1)}+A_n^{(2a)}+A_n^{(2b)} \tag{16}$$

containing the internuclear terms is evaluated in this section. For the first-order term, if the bound-state wave functions are Fourier analyzed, then the operation of $\widetilde{\mathscr{T}}_{PT}$ on the $\mathbf{r}$ plane wave, along with the use of the $\delta$ function arising from the $\mathbf{r}$ integration (which forces $\mathbf{k}_f=\mathbf{k}_i-\mathbf{v}$ to order $m/M_P$ and $m/M_T$) for performing the $\mathbf{k}_f$ integration, gives

$$A_n^{(1)}=\int d\mathbf{k}_i\ \widetilde{\phi}_f(\mathbf{k}_i-\mathbf{v})^*\widetilde{\phi}_i(\mathbf{k}_i)T_{PT}(\mathbf{U}_i-\mathbf{k}_i-\mathbf{J},\mathbf{U}_i;E_n), \tag{17}$$

where $\mathbf{U}_i=(1-\gamma)\mathbf{k}_i+[1-(1-\gamma)(1-\alpha)]\mathbf{K}_i$ and $E_n=E-[\mathbf{k}_i-(1-\alpha)\mathbf{K}_i]^2/2\nu_n$.

For the first of the second-order terms in Eq. (16), letting $\widetilde{\mathscr{T}}_{Te}$ and $G_o^+$ operate to the left on the $\mathbf{R}_T$ plane wave and $\widetilde{\mathscr{T}}_{PT}$ operate to the right on the $\mathbf{r}$ plane wave and inserting complete sets of plane-wave states in $\mathbf{r}$ and $\mathbf{R}$ between $G_o^+$ and $\widetilde{\mathscr{T}}_{PT}$, one derives the expression

$$A_n^{(2a)}=(2\pi)^{-3}\int d\mathbf{k}_f d\mathbf{k}_i\ \widetilde{\phi}_f(\mathbf{k}_f)^*\widetilde{\phi}_i(\mathbf{k}_i)\times T_{Te}(\mathbf{k}_f+\mathbf{v},\mathbf{k}_i-(1-\alpha)(\mathbf{k}_f-\mathbf{K});E_f)\widetilde{G}_o^+(E_f)\times T_{PT}(\mathbf{U}_i-\mathbf{k}_f-\mathbf{K},\mathbf{U}_i;E_n). \tag{18}$$

The $\delta$ functions arising from the $\mathbf{r}$ and $\mathbf{R}$ integrations have been used to evaluate the integrals of the complete sets. The momentum-space Green function in this expression is given by

$$\widetilde{G}_o^+(E_f)=\left\{E_f-\frac{1}{2\mu_i}[\mathbf{k}_i+(1-\alpha)(\mathbf{K}-\mathbf{k}_f)]^2+i\eta\right\}^{-1}. \tag{19}$$

Similarly, for the second of the second-order terms in Eq. (16), one finds

$$A_n^{(2b)}=(2\pi)^{-3}\int d\mathbf{k}_f d\mathbf{k}_i\ \widetilde{\phi}_f(\mathbf{k}_f)^*\widetilde{\phi}_i(\mathbf{k}_i)\times T_{PT}(\mathbf{U}_f,\mathbf{U}_f+\mathbf{k}_i+\mathbf{J};E_n)\widetilde{G}_o^+(E_i)\times T_{Pe}(-\mathbf{k}_f+(1-\beta)(\mathbf{k}_i+\mathbf{J}),\mathbf{k}_i+\mathbf{v};E_i), \tag{20}$$

with $\mathbf{U}_f=-\gamma\mathbf{k}_f+[1-\gamma(1-\beta)]\mathbf{K}_f$. The free Green function here has the form

$$\widetilde{G}_o^+(E_i)=\left\{E_i-\frac{1}{2\mu_f}[-\mathbf{k}_f+(1-\beta)(\mathbf{k}_i+\mathbf{J})]^2+i\eta\right\}^{-1} \tag{21}$$

in momentum space.

## III. EVALUATION AND MODIFICATION OF THE AMPLITUDE

### A. Near-shell approximation for a screened potential

It has been shown for singly charged ions incident on neutral atoms that the total amplitude $A_{F2}$ is well-behaved: nonintegrable singularities are not present. Therefore, approximations to it can be made. In this section, near-shell forms of the two-body transition matrices are used that introduce errors of the order of the squares of the ratios of the projectile and target-nuclear charges to the impact velocity; that is, the partial amplitude of $A_{F2}$ given in Eq. (12) is approximated to order $(Z_P/v)^2$ and $(Z_T/v)^2$.

While it is true that corrections to the near-shell approximation will be expected to be larger at lower energies, it is apparent from Figs. 7(a) and 7(b) (discussed below in Sec. IV) that the second-order contribution is also relatively smaller, making the near-shell corrections less important. Contributing to this are the large first Born contribution [see after Eq. (10)] and the incorporation of the electronic scattering normalization, detailed below in Sec. III E.

For modified Coulomb potentials, the two-body transition matrix reduces to a generalized elastic-scattering amplitude multiplied by a so-called off-energy-shell factor when the energy shell is approached. The amplitude is the sum of an amplitude for the Coulomb potential and an amplitude for the short-range part of the potential. Because of the presence of the bound-state wave functions, the integral in the second-order electronic term is dominated by momentum values in the regions $k_i\lesssim Z_T$ and $k_f\lesssim Z_P$. Following previous work on modified Coulomb potentials [12] that extends the result of Chen and Chen [16] on pure Coulomb scattering, the approximation near the energy shell to the two-body scattering matrix for a screened potential is found to be

$$T_{MC}(\mathbf{k}',\mathbf{k};\varepsilon)\approx-2\pi g^+(Z^\infty,k',\varepsilon)g^+(Z^\infty,k,\varepsilon)\times[f^{C\infty}_{\mathbf{k}',\mathbf{k}}(\varepsilon)+f^{SR}_{\mathbf{k}',\mathbf{k}}(\varepsilon)], \tag{22}$$

where the off-shell factor is defined as

$$g^\pm(Z^\infty,k,\kappa)=e^{\pi\nu^\infty/2}\Gamma(1\mp i\nu^\infty)\left[\frac{k-\kappa}{k+\kappa}\right]^{\mp i\nu^\infty} \tag{23}$$

and where $\nu^\infty\equiv Z^\infty/\kappa$, $\kappa\equiv(2\mu\varepsilon+i\eta)^{1/2}$, $\mu$ is the reduced mass, and $\Gamma(x)$ is the gamma function.

Scattering in the asymptotic Coulomb-field of charge $Z^\infty$ is measured by the Coulomb scattering amplitude

$$f^{C\infty}_{\mathbf{k}',\mathbf{k}}(\varepsilon)=\frac{2Z^\infty}{|\mathbf{k}'-\mathbf{k}|^2}e^{2i\sigma_0}\left[\frac{|\mathbf{k}'-\mathbf{k}|}{k'+k}\right]^{2i\nu^\infty}, \tag{24}$$

with $\sigma_0=\arg\Gamma(1-i\nu^\infty)$. Relative to the asymptotic Coulomb scattering, the additional scattering in the short-range part of the potential is measured by the amplitude

$$f^{SR}_{\mathbf{k}',\mathbf{k}}(\varepsilon)=\frac{\kappa}{kk'}\sum_{l=0}^{\infty}(2l+1)e^{i(2\sigma_l+\delta_l)}\sin\delta_l\ P_l(\hat{\mathbf{k}}'\cdot\hat{\mathbf{k}}), \tag{25}$$

with $\delta_l$ the phase shift for the short-range potential [7].

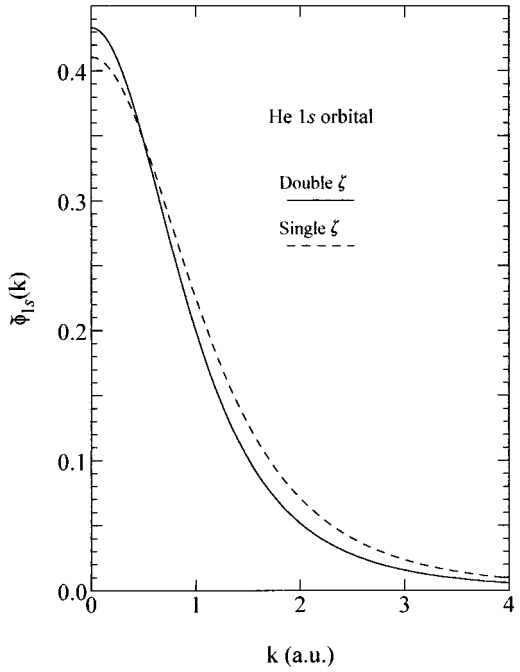


FIG. 1. Single- and double-$\zeta$ Hartree-Fock 1$s$ orbitals in momentum space.

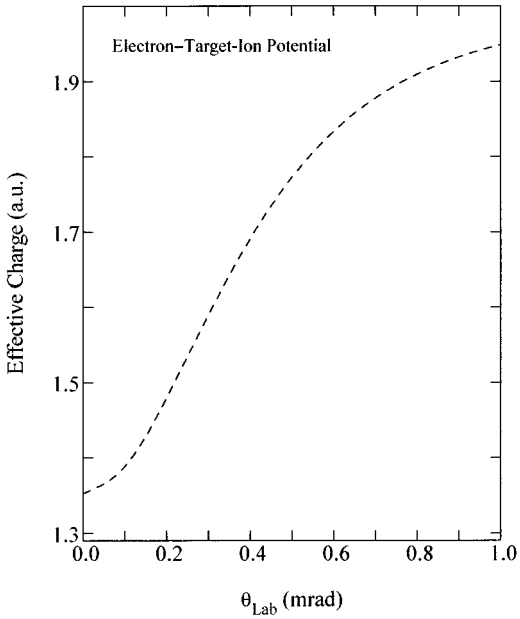


FIG. 2. Effective charge, defined as $-k^2V_{HF}(k)$, for the screened potential derived from the Hartree-Fock 1$s$ target orbital versus $k$.

In the present application for the electron–target-ion potential only the $l=0$ component of the short-range amplitude is retained. Manson has compiled phase shifts [17] for an electron scattering in an unrelaxed Herman-Skillman (Hartree-Fock-Slater) potential [18] for the ground state of a large sequence of atoms. Extrapolating in impact energy his value for helium, the value $\delta_0=0.3860$ is obtained. This value is used here. The value for $\delta_1$ is at least a factor of 5 smaller than $\delta_0$. Consequently, the phase shifts $\delta_n$, for $n>0$, are not used.

### B. Helium wave function and screened potential

Since the single-$\zeta$ ground-state wave function of helium weights radial values differently than more accurate wave functions, it follows that momentum components will likewise be weighted differently. Since the amplitude involves an integration over the momentum distribution, results could also be affected.

To study this possibility, the ground-state wave function is represented by a double-$\zeta$ function [6]

$$\phi_i(\mathbf{r})=\{c_1N_1e^{-\zeta_1 r}+c_2N_2e^{-\zeta_2 r}\}Y_{00}(\hat{\mathbf{r}}), \tag{26}$$

with $c_1=0.18069$, $c_2=0.84378$, $\zeta_1=2.91093$, $\zeta_2=1.45363$, $N_j=2\zeta_j^{3/2}$ $(j=1,2)$, and $Y_{00}=1/\sqrt{4\pi}$. The orbital energy of this state is $-24.978$ eV, and the corresponding total energy is $-77.868$ eV, which is within $2\times10^{-5}$ eV of the Hartree-Fock limit. The experimental energy is $-78.975$ eV. In momentum space Eq. (26) takes the form

$$\tilde{\phi}_i(\mathbf{k})=\{c_1\tilde{N}_1(k^2+\zeta_1^2)^{-2}+c_2\tilde{N}_2(k^2+\zeta_2^2)^{-2}\}Y_{00}(\hat{\mathbf{k}}), \tag{27}$$

where $\tilde{N}_j=(2^5\zeta_j^5/\pi)^{1/2}$ $(j=1,2)$. Figure 1 shows the single- and double-$\zeta$ wave functions in momentum space. It is seen that the better wave function is more peaked than the other more approximate one. The effect of this on the cross section is studied below.

While considerably more sophisticated helium wave functions are available, the double-$\zeta$ function is used because the effect on the cross section of using a better wave function can still be investigated with a minimal impact on computational complexity. The two exponents bracket the single-$\zeta$ value of 1.6875 and both of the coefficients are positive. The relatively large value of $\zeta_1$ means that, in particular, the inner form of the initial bound-state charge distribution is better represented.

With this wave function, an unrelaxed atomic potential can be obtained that is derived from the sum of the electron-nucleus attraction and the average electron-electron repulsion:

$$V_{HF}(\mathbf{r})=\int d\mathbf{r}'[-Z_T\delta(\mathbf{r}')+|\phi_i(\mathbf{r}')|^2]|\mathbf{r}-\mathbf{r}'|^{-1}. \tag{28}$$

Using the Fourier transform $\tilde{V}_{HF}(\mathbf{k})$ of this potential, a charge for a scaled Coulomb potential can be defined as

$$\tilde{V}_{HF}(k)\equiv-\left(\frac{2}{\pi}\right)^{1/2}\frac{Z_s(k)}{k^2}, \tag{29}$$

where $Z_s$ is dependent on the momentum transfer. Due to the spherical nature of the ground-state wave function Eq. (26), $\tilde{V}_{HF}$ depends only on $k$. The behavior of $Z_s(k)$ versus $k$ is shown in Fig. 2, where a smooth transition from a charge of about 1 for projectile scattering angles near 0 mrad to about 2 at 1 mrad is seen. This behavior reflects the increasing penetration of the target ion by the projectile.

Since the modified Coulomb potential is well represented by a scaled pure Coulomb potential of charge $Z_s$ in the inner

region, the sum of the Coulomb and short-range amplitudes is approximated by the Coulomb amplitude for the screened potential,

$$f^{C}_{\mathbf{k}',\mathbf{k}}(\varepsilon)=\frac{2Z_s}{|\mathbf{k}'-\mathbf{k}|^2}e^{2i\sigma_0}\left[\frac{|\mathbf{k}'-\mathbf{k}|}{k'+k}\right]^{2i\nu_s}, \tag{30}$$

with $\nu_s=\mu Z_s/(2\mu\varepsilon+i\eta)^{1/2}$ here. Such a simplification works when the impact energies are large, so that the individual collisions in the double scatterings are hard collisions and the momentum transfers are large. A comparison of this amplitude with the amplitude $f^{C\infty}_{\mathbf{k}',\mathbf{k}}(\varepsilon)+f^{SR}_{\mathbf{k}',\mathbf{k}}(\varepsilon)$ in the above noted $l=0$ approximation is shown in Fig. 3. Little difference is seen in the real component (a), whereas the imaginary component (b) is underestimated grossly by the effective amplitude.

### C. Evaluation of the electronic amplitude

The near-shell approximations to the electronic-nuclear transition matrices in $A^{(2)}_e$ are

$$T_{Pe}(\mathbf{k}_f+\mathbf{k}_i+\mathbf{J},\mathbf{k}_i-\mathbf{v};E_i)$$
$$\approx -4\pi e^{\pi\nu_P^\infty}\frac{\Gamma(1+i\nu_P^\infty)^2\Gamma(1-i\nu_P)}{\Gamma(1+i\nu_P)}$$
$$\times\left\{\frac{k_i^2-2\varepsilon_i}{(8E_i)^2\widetilde{G}_o^+}\right\}^{-i\nu_P^\infty}\frac{Z_P}{|\mathbf{k}_f-\mathbf{K}|^2}\left\{\frac{|\mathbf{k}_f-\mathbf{K}|^2}{8E_i}\right\}^{i\nu_P} \tag{31}$$

and

$$T_{Te}(\mathbf{k}_f+\mathbf{v},\mathbf{k}_i+\mathbf{k}_f-\mathbf{K};E_f)$$
$$=-4\pi e^{\pi\nu_T^\infty}|\Gamma(1+i\nu_T^\infty)|^2\left[\frac{k_f^2-2\varepsilon_f}{(8E_f)^2\widetilde{G}_o^+}\right]^{-i\nu_T^\infty}$$
$$\times\left\{\frac{Z_T^\infty}{|\mathbf{k}_i+\mathbf{J}|^2}\left(\frac{|\mathbf{k}_i+\mathbf{J}|^2}{8E_f}\right)^{i\nu_T^\infty}+\frac{(2E_f)^{1/2}e^{i\delta_0}\sin\delta_0}{2|\mathbf{k}_f+\mathbf{v}||\mathbf{k}_i+\mathbf{k}_f-\mathbf{K}|}\right\}. \tag{32}$$

Using these expressions, neglecting the slowly varying $\mathbf{k}_i$ and $\mathbf{k}_f$ dependences of the integrand, and introducing the $1s$ bound-state wave function, the amplitude becomes

$$A_e^2=2(2/\pi)^3Z_P(Z_TZ_P)^{5/2}e^{\pi\nu_P^\infty}\frac{\Gamma(1+i\nu_P^\infty)^2\Gamma(1-i\nu_P)}{\Gamma(1+i\nu_P)}(4v^2)^{i(2\nu_P^\infty-\nu_P)}K^{-2+2i\nu_P}e^{\pi\nu_T^\infty}|\Gamma(1+i\nu_T^\infty)|^2(4v^2)^{2i\nu_T^\infty}$$
$$\times\left[\frac{Z_T^\infty}{J^2}\left(\frac{J}{2v}\right)^{2i\nu_T^\infty}+\frac{e^{i\delta_0}\sin\delta_0}{2K}\right]\int d\mathbf{k}_f d\mathbf{k}_i\,(k_i^2-2\varepsilon_i)^{-2-i\nu_P^\infty}(k_f^2-2\varepsilon_f)^{-2-i\nu_T^\infty}[\widetilde{G}_S^+(E_i)]^{1+i\nu_T^\infty+i\nu_P^\infty}, \tag{33}$$

with the Sommerfeld parameters defined as

$$\nu_P^\infty=Z_P^\infty/v,\quad \nu_P=Z_P/v,\quad \nu_T^\infty=Z_T^\infty/v,\quad \nu_T=Z_T/v. \tag{34}$$

In Eq. (33), the free Green function Eq. (15) is approximated as

$$\widetilde{G}_S^+(E_i)\equiv[\tfrac{1}{2}(v^2-K^2+\varepsilon_i)-\mathbf{k}_f\cdot\mathbf{J}+\mathbf{k}_i\cdot\mathbf{K}$$
$$-\tfrac{1}{2}(k_i^2+k_f^2)+i\eta]^{-1}, \tag{35}$$

where advantage is taken of the spherical symmetry of the initial and final bound-state wave functions to uniformly ''average'' the *direction* of $\mathbf{k}_f$ relative to $\mathbf{k}_i$ and write $(\mathbf{k}_i-\mathbf{k}_f)^2\approx k_i^2+k_f^2$. However, the quadratic dependence of the free Green-function on the momentum variables is retained [14].

The six-dimensional integral in Eq. (33) is evaluated as in previous work [1]. Briefly, the angular integrations over $\hat{\mathbf{k}}_i$ and $\hat{\mathbf{k}}_f$ are performed straightforwardly. The radial variables $k_i$ and $k_f$ are then expressed in polar coordinates. Using Cauchy's integral theorem, the integration path for $k_\rho$ along the positive real axis is transformed to a path off the real axis to avoid the Green-function singularity. Tolerances were given as $10^{-8}$ and $10^{-6}$, respectively, for the angular $k_\theta$ and radial $k_\rho$ integrations, which are carried out using the adaptive eight-panel Newton-Cotes quadrature. The output of the cross sections was explicitly checked to assure better than a four digit accuracy.

### D. Evaluation of the internuclear amplitude

The near-shell approximation to the transition matrix for the first-order internuclear term Eq. (17) is

$$T_{PT}(\mathbf{U}_i-\mathbf{k}_i-\mathbf{J},\mathbf{U}_i;E_n)$$
$$\approx 4\pi e^{-\pi\nu_{PT}^\infty}\frac{\Gamma(1-i\nu_{PT}^\infty)^2\Gamma(1+i\nu_{PT})}{\Gamma(1-i\nu_{PT})}$$
$$\times\left(\frac{[(\mathbf{k}_i-\mathbf{v})^2-2\varepsilon_f][k_i^2-2\varepsilon_i]}{(8E_n)^2}\right)^{i\nu_{PT}^\infty}\frac{Z_PZ_T}{|\mathbf{k}_i+\mathbf{J}|^2}$$
$$\times\left(\frac{|\mathbf{k}_i+\mathbf{J}|^2}{8\mu_nE_n}\right)^{-i\nu_{PT}}, \tag{36}$$

with $\nu_{PT}^\infty=\mu_nZ_P^\infty Z_T^\infty/(2\mu_nE_n)^{1/2}$ and $\nu_{PT}=\mu_nZ_PZ_T/(2\mu_nE_n)^{1/2}$. The reduced mass $\mu_n$ factor does not cancel in this expression because the inner and outer charges of the modified Coulomb potential are different.

The remaining integral is evaluated by treating the two dominant peaks in the integrand at $\mathbf{k}_i=\mathbf{0}$ and $\mathbf{k}_i=\mathbf{v}$ as independent, with the slow $\mathbf{k}_i$ variation of the other factors about

the peaks being neglected. This is justified if the two peaks are well separated in momentum space, as is true for $v \gg Z_P$ and $v \gg Z_T$.

The transition matrix approximations to the term in Eq. (18) are

$$T_{PT}(\mathbf{U}_i-\mathbf{k}_f+\mathbf{K},\mathbf{U}_i;E_n)$$
$$\approx 4\pi e^{-\pi\nu_{PT}^{\infty}}\frac{\Gamma(1-i\nu_{PT}^{\infty})^2\Gamma(1+i\nu_{PT})}{\Gamma(1-i\nu_{PT})}\left(\frac{k_i^2-2\varepsilon_i}{8E_n}\right)^{i\nu_{PT}^{\infty}}$$
$$\times(8E_n\tilde{G}_o^{+})^{-i\nu_{PT}^{\infty}}\frac{Z_PZ_T}{|\mathbf{k}_f-\mathbf{K}|^2}\left(\frac{|\mathbf{k}_f-\mathbf{K}|^2}{8\mu_nE_n}\right)^{-i\nu_{PT}} \quad (37)$$

and

$$T_{Te}(\mathbf{k}_f+\mathbf{v},\mathbf{k}_i;E_f)$$
$$\approx -4\pi e^{\pi\nu_T^{\infty}}\frac{\Gamma(1+i\nu_T^{\infty})^2\Gamma(1-i\nu_T)}{\Gamma(1+i\nu_T)}\left(\frac{k_f^2-2\varepsilon_f}{8E_f}\right)^{-i\nu_T^{\infty}}$$
$$\times\left(\frac{k_i-\sqrt{2E_f}}{k_i+\sqrt{2E_f}}\right)^{-i\nu_T^{\infty}}\frac{Z_T}{|\mathbf{k}_f-\mathbf{k}_i+\mathbf{v}|^2}$$
$$\times\left(\frac{|\mathbf{k}_f-\mathbf{k}_i+\mathbf{v}|^2}{(|\mathbf{k}_f+\mathbf{v}|+k_i)^2}\right)^{i\nu_T}, \quad (38)$$

where $\nu_T^{\infty}=Z_T^{\infty}/(2E_f)^{1/2}$ and $\nu_T=Z_T/(2E_f)^{1/2}$.

The transition matrix approximations to the other second-order internuclear term in Eq. (20) are

$$T_{PT}(\mathbf{U}_f,\mathbf{U}_f+\mathbf{k}_i+\mathbf{J};E_n)$$
$$\approx 4\pi e^{-\pi\nu_{PT}^{\infty}}\frac{\Gamma(1-i\nu_{PT}^{\infty})^2\Gamma(1+i\nu_{PT})}{\Gamma(1-i\nu_{PT})}\left(\frac{k_f^2-2\varepsilon_f}{8E_n}\right)^{i\nu_{PT}^{\infty}}$$
$$\times(8E_n\tilde{G}_o^{+})^{-i\nu_{PT}^{\infty}}\frac{Z_PZ_T}{|\mathbf{k}_i+\mathbf{J}|^2}\left(\frac{|\mathbf{k}_i+\mathbf{J}|^2}{8\mu_nE_n}\right)^{-i\nu_{PT}} \quad (39)$$

and

$$T_{Pe}(-\mathbf{k}_f,\mathbf{k}_i-\mathbf{v};E_i)$$
$$\approx -4\pi e^{\pi\nu_P^{\infty}}\frac{\Gamma(1+i\nu_P^{\infty})^2\Gamma(1-i\nu_P)}{\Gamma(1+i\nu_P)}\left(\frac{k_i^2-2\varepsilon_i}{8E_i}\right)^{-i\nu_P^{\infty}}$$
$$\times\left(\frac{k_f-\sqrt{2E_i}}{k_f+\sqrt{2E_i}}\right)^{-i\nu_P^{\infty}}\frac{Z_P}{|\mathbf{k}_i+\mathbf{k}_f-\mathbf{v}|^2}$$
$$\times\left(\frac{|\mathbf{k}_i+\mathbf{k}_f-\mathbf{v}|^2}{(|\mathbf{k}_i-\mathbf{v}|+k_f)^2}\right)^{i\nu_P}, \quad (40)$$

where $\nu_P^{\infty}=Z_P^{\infty}/(2E_i)^{1/2}$ and $\nu_P=Z_P/(2E_i)^{1/2}$.

Retaining only those terms in the integrand in which the momentum variation is rapid, performing the $\mathbf{k}_i$ and $\mathbf{k}_f$ integrations, combining the results, and regrouping factors, one finds

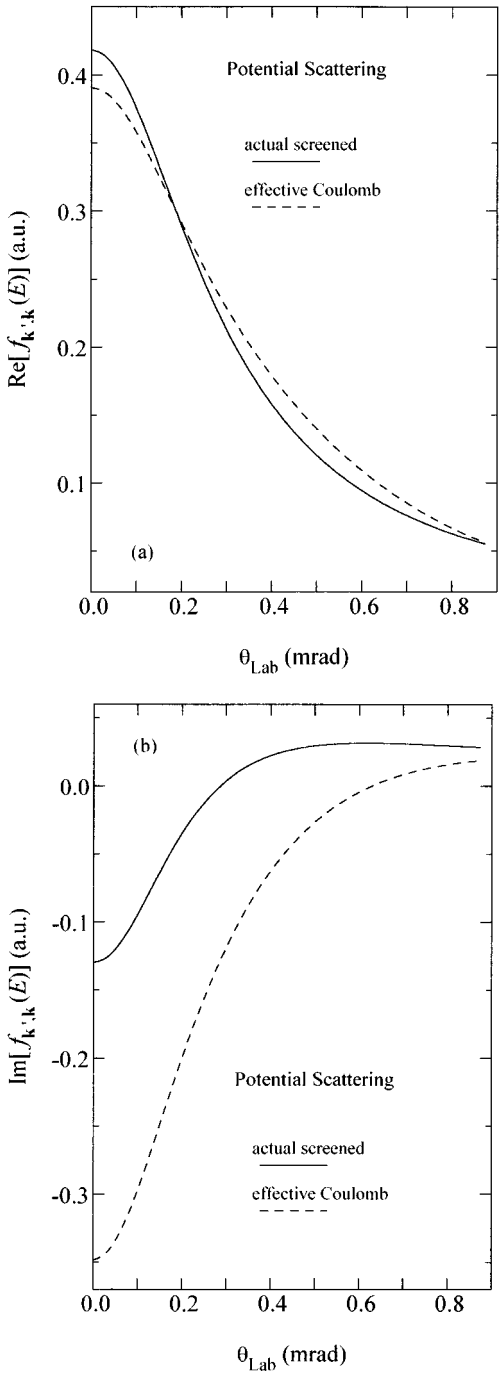


FIG. 3. Real (a) and imaginary (b) parts of the two-body scattering amplitude $f_{\mathbf{k}',\mathbf{k}}(E)$ for the screened target potential versus laboratory scattering angle, which is related to $|\mathbf{k}'-\mathbf{k}|$.

$$A_n=S_{PT}f_n^C(K)+S_{TP}f_n^C(J), \quad (41)$$

with the internuclear-scattering amplitude defined by

$$f_n^C(Q)=-\frac{2Z_PZ_T}{Q^2}\frac{\Gamma(1+i\nu_{PT})}{\Gamma(1-i\nu_{PT})}\left(\frac{Q}{2\mu_nv}\right)^{+2i\nu_{PT}}. \quad (42)$$

The constant $S_{PT}$, which is independent of $J$ and $K$, is given by

$$S_{PT}=2^5\pi Z_T(Z_PZ_T)^{3/2}e^{-\pi\nu_{PT}^{\infty}}\frac{\Gamma(1-i\nu_{PT}^{\infty})\Gamma(\frac{1}{2}-i\nu_{PT}^{\infty})}{(1-i\nu_{PT}^{\infty})\sqrt{\pi}}(4\mu_n v^2)^{-2i\nu_{PT}^{\infty}}$$
$$\times\left[Z_P^{2i\nu_{PT}^{\infty}}(v^2+Z_T^2)^{-2+i\nu_{PT}^{\infty}}-\tfrac{1}{2}Z_T^{2i\nu_{PT}^{\infty}}\frac{\Gamma(\frac{1}{2}+i\nu_T^{\infty})\Gamma(1+i\nu_T^{\infty})\Gamma(1-i\nu_T)}{(1+i\nu_T^{\infty})\sqrt{\pi}\Gamma(1+i\nu_T)}\left(\frac{Z_P}{2v}\right)^{-2i\nu_T^{\infty}}v^{-2+2i\nu_T}\left(\frac{v^2-Z_P^2}{2}\right)^{-1+i\nu_{PT}^{\infty}}\right]. \tag{43}$$

$S_{TP}$ is obtained from $S_{PT}$ by the change $P\leftrightarrow T$, where $\nu_T^{\infty}$, $\nu_T$, $\nu_P^{\infty}$, and $\nu_P$ are given by Eqs. (34) and where now $\nu_{PT}^{\infty}=Z_P^{\infty}Z_T^{\infty}/v$ and $\nu_{PT}=Z_PZ_T/v$.

Equation (41) is symmetric in the two charges and in the momentum transfers. The dependences on $K^{-2}$ and $J^{-2}$ reflect the nuclear Coulomb scattering. Also noteworthy is the appearance of two terms of opposite sign in each set of large parentheses. Ignoring the different multiplying factors and neglecting factors of order $(Z_P/v)^2$ and $(Z_T/v)^2$, a cancellation of contributions is expected in Eq. (43) (and $S_{TP}$). Indeed, for the second-order Born approximation, which is obtained by setting all of the Sommerfeld parameters equal to zero, the cancellation leads to a vanishing contribution.

The eikonal treatment of the internuclear contribution to forward-angle capture [9] consists of Bessel transforming the given electronic amplitude $A_e(K_\perp)$ [Eqs. (10) and (33)], as a function of transverse momentum transfer $K_\perp$, to impact-parameter space $b$:

$$a_e(b)=\int_0^{\infty}dK_\perp K_\perp J_0(bK_\perp)A_e(K_\perp), \tag{44}$$

multiplying $a_e(b)$ by the eikonal phase factor $e^{2i\nu_{PT}}$, and then transforming the result back to momentum-transfer space

$$A_{e+n}(K_\perp)=\int_0^{\infty}db\ b^{1+2i\nu_{PT}}J_0(K_\perp b)a_e(b), \tag{45}$$

where $\nu_{PT}$ is the previously defined internuclear Sommerfeld parameter. In Eq. (45) for $A_{e+n}$, the electronic and nuclear contributions are mixed together. Normalization of the double integration must be consistent with the definition of the amplitude relative to its use in the differential cross section and is easily checked by setting $\nu_{PT}=0$ and comparing the doubly transformed amplitude with the untransformed amplitude. This latter procedure also provides a gauge of the accuracy of the numerical quadratures. As a further check on errors arising from the imperfectly calculated amplitude, which is read in at a tabulated set of values, the double numerical quadrature was performed on the analytic function $\{c+K_\perp^2\}^{-2}$.

Neither of the internuclear contributions above lead to results which agree well with the experimental data over the whole of the angular region. This comparison is shown below in Fig. 6 of Sec. IV. To correct this situation, which most likely arises from the limitations in the evaluation of the internuclear amplitude, Eq. (41) is normalized to the amplitude given by Eq. (45) at the scattering angle 1.2 mrad, where only the internuclear part contributes. The electronic part of the amplitude is left unaltered.

### E. Normalization of the electronic scattering

The wave packets representing the virtual scattering of the electron in the initial and final channels make use of the off-shell scattering states that appear implicitly in the transition matrices in Eq. (12) and are defined by Eq. (14). As Marxer and Briggs have noted, the wave packets can lose normalization [8]; their procedure for normalizing them is employed here.

The relevant wave packets are defined as

$$\xi_{\mathbf{v},i}^{+}(\mathbf{r}_P)\equiv\int d\mathbf{k}\ \tilde{\phi}_i(\mathbf{k})\psi_{\varepsilon,\mathbf{v}-\mathbf{k}}^{+}(\mathbf{r}_P)$$

and

$$\xi_{\mathbf{v},f}^{-}(\mathbf{r}_T)\equiv\int d\mathbf{k}\ \tilde{\phi}_f(\mathbf{k})\psi_{\varepsilon,\mathbf{v}+\mathbf{k}}^{-}(\mathbf{r}_T),$$

where $\varepsilon$ is a function of $\mathbf{k}$, $\varepsilon(\mathbf{k})$. These wave packets are normalized according to whether the square roots of the integrals over all space of the squares of the wave packets, viz.,

$$N_i(v)=(\langle\xi_{\mathbf{v},i}^{+}|\xi_{\mathbf{v},i}^{+}\rangle)^{1/2} \tag{46}$$

and

$$N_f(v)=(\langle\xi_{\mathbf{v},f}^{-}|\xi_{\mathbf{v},f}^{-}\rangle)^{1/2}, \tag{47}$$

are unity. In Eqs. (46) and (47), the dependences on the initial or final bound-state wave functions and on the velocity are noted explicitly.

Considering $\xi_{\mathbf{v},f}^{-}$, the relevant interaction region, which is centered around the target nucleus $r_T\lesssim Z_T$, implies that the off-shell wave function $\psi_{\varepsilon,\mathbf{q}}^{-}(\mathbf{r}_T)$ can be approximated [12] to order $(Z_P/v)^2$ by a target continuum eigenstate $\psi_{\mathbf{q}}^{-}(\mathbf{r}_T)$ multiplied by an off-shell factor:

$$\psi_{\varepsilon,\mathbf{q}}^{-}(\mathbf{r}_T)\approx g^{-}(Z_T^{\infty},q,\kappa)\psi_{\mathbf{q}}^{-}(\mathbf{r}_T) \tag{48}$$

for $\varepsilon\equiv\frac{1}{2}\kappa^2\approx\frac{1}{2}q^2$. As noted earlier, this approximation holds for centrally modified Coulomb potentials. The wave function $\phi_i$ in the matrix element ensures the validity of the approximation. The factor $g^{-}$ has been defined above in Eq. (23). Here, the charge dependence of the asymptotic form of the target potential means that $Z^{\infty}=Z_T^{\infty}$. An analogous argument can be made for $\xi_{\mathbf{v},i}^{+}$.

Employing the near-shell approximations for the off-energy-shell scattering wave functions and making use of the orthonormality of the eigenfunctions $\psi_{\mathbf{q}}^{+}(\mathbf{r})$, one obtains

$$N_i(v)\approx\left(\int d\mathbf{k}|\tilde{\phi}_i(\mathbf{k})|^2|g^+(Z_P^\infty,q,\kappa)|^2\right)^{1/2} \tag{49}$$

and

$$N_f(v)\approx\left(\int d\mathbf{k}|\tilde{\phi}_f(\mathbf{k})|^2|g^-(Z_T^\infty,q,\kappa)|^2\right)^{1/2}. \tag{50}$$

Noting Eq. (23), it is seen that the rapidly varying parts of $g^{\pm}$ are canceled by $(g^{\pm})^*$. Thus, since $|\tilde{\phi}_i(\mathbf{k})|^2$ and $|\tilde{\phi}_f(\mathbf{k})|^2$ are *highly* localized about $\mathbf{k}=\mathbf{0}$, accurate approximations can be made:

$$N_i(v)\approx|g^+(Z_P^\infty,q,\kappa)|_{\mathbf{k}=\mathbf{0}}\left(\int d\mathbf{k}|\tilde{\phi}_i(\mathbf{k})|^2\right)^{1/2}$$

$$=\left(\frac{2\pi\nu_P^\infty}{1-e^{-2\pi\nu_P^\infty}}\right)^{1/2} \tag{51}$$

and

$$N_f(v)\approx|g^-(Z_T^\infty,q,\kappa)|_{\mathbf{k}=\mathbf{0}}\left(\int d\mathbf{k}|\tilde{\phi}_f(\mathbf{k})|^2\right)^{1/2}$$

$$=\left(\frac{2\pi\nu_T^\infty}{1-e^{-2\pi\nu_T^\infty}}\right)^{1/2}, \tag{52}$$

where $\nu_P^\infty=Z_P^\infty/(v^2-2\varepsilon_i)^{1/2}$ and $\nu_T^\infty=Z_T^\infty/(v^2-2\varepsilon_f)^{1/2}$.

For high velocities, $N_i\approx1+\pi\nu_P^\infty/2$ and $N_f\approx1+\pi\nu_T^\infty/2$, showing that the normalizations approach unity. For lower velocities, however, the corrections can become significant. In the present case, $2\pi\nu_P^\infty=1.917$ and $2\pi\nu_T^\infty=2.107$, and $[N_i(v)]^{-1}=0.6670$ and $[N_f(v)]^{-1}=0.6457$. The product is then $[N_i(v)N_f(v)]^{-1}=0.4307$. Since $N_i$ and $N_f$ are not equal to unity, the scattering states are corrected (renormalized). The use of $N_iN_f$ also reduces the importance of near-shell corrections at lower velocity [8].

## IV. RESULTS AND DISCUSSION

Results calculated using the modified second-order Faddeev formalism are compared first with other theoretical results and with the experimental results. An analysis is then made of the effect on the cross section of the various refinements to the amplitude. Differential cross sections for electron capture in proton-helium collisions at 293 keV are presented in Fig. 4. The calculated $1s\rightarrow1s$ results are obtained using the present modified second-order Faddeev approximation [i.e., the sum of $A_e$ in Eq. (33) and $A_n$ in Eq. (41)], the two-state atomic expansion of Lin and Soong [10], and the continuum distorted-wave approximation of Rivarola *et al.* [11]. The experimental results of Bratton, Cocke, and Macdonald [5] include capture into all final states. First Born (Brinkman-Kramers) results of Rogers and McGuire [20] are not shown, as they are generally a factor 3.5 too large. In the Faddeev calculations, the values assumed for the charges in the Sommerfeld parameters are $Z_P=Z_P^\infty=1.0$, $Z_T=1.6875$, and $Z_T^\infty=1.0$. The agreement in magnitude and shape of the Faddeev cross section with the experimental data and with the two-state results is generally very good for the entire angular range considered. For angles up to 0.6 mrad, the agreement appears to be especially good; however, the inclusion of the excited-state contribution could lead to results that are too large. In the 0.6–0.8 mrad region the Faddeev results are slightly too large, and the shape too flat. The CDW results are too small for angles below 0.2 mrad and have a dip in 0.7–1.0 mrad region not present in the experimental results.

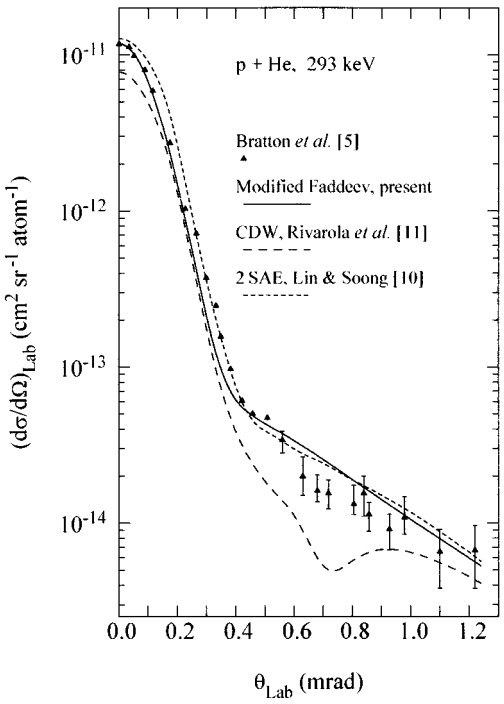


FIG. 4. Differential cross section for $1s\rightarrow1s$ electron capture in 293 keV proton-helium collisions: modified second-order Faddeev approximation, present calculation; experimental data, Bratton, Cocke, and Macdonald [5]; two-state atomic expansion, Lin and Soong [10]; continuum distorted-wave approximation, Rivarola *et al.* [11]. The experimental results include capture into all final states.

In Fig. 5, Faddeev cross sections obtained using various approximations with the internuclear contribution omitted are compared among themselves over the angular region where the electronic amplitude contributes appreciably. This figure shows the relative importance of the individual corrections. The cross section derived from a single-$\zeta$ helium wave function shows small differences with the one derived from the double-$\zeta$ wave function, being roughly 5% larger at 0.0 mrad and up to 5% smaller at 0.5 mrad. Thus, the form of the bound-state wave function has a minimal effect on the amplitude calculation. (The effect is largest in the two regions where the most cancellation occurs among the various partial amplitudes—first Born, second-order electronic, and internuclear.) The use of an amplitude derived using an effective Coulomb potential with a scaled (screened) charge [Eqs. (29) and (30)] instead of the amplitude with the actual screened potential, however, leads to larger differences. For angles

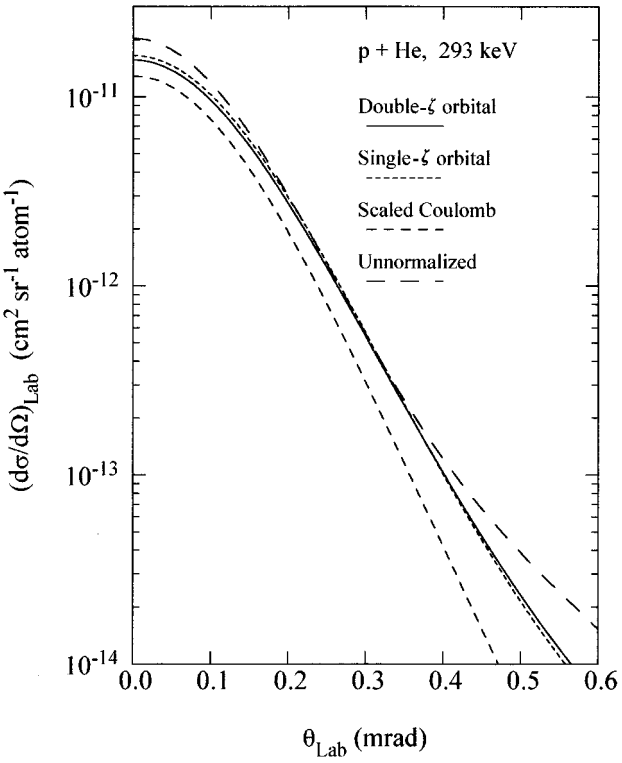


FIG. 5. Differential capture cross sections obtained with the modified Faddeev approximation employing single- or double-$\zeta$ helium wave functions or a two-body scattering amplitude derived from an effective Coulomb approximation to the actual electron–target-ion potential or unnormalized electronic scattering states, all with the internuclear contribution omitted.

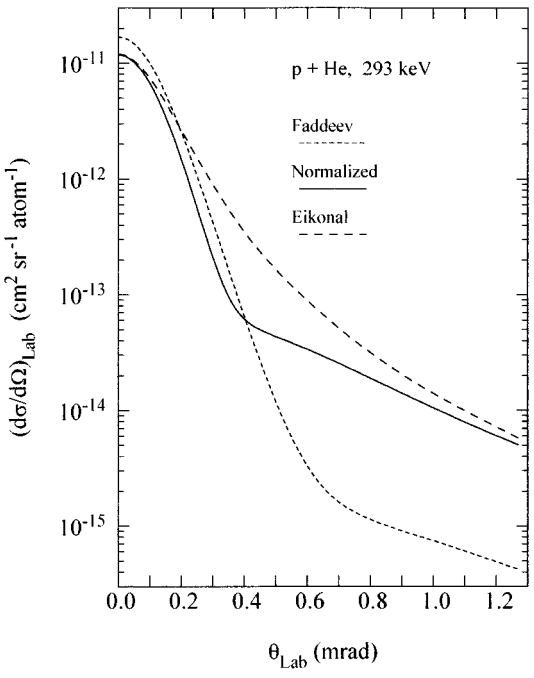


FIG. 6. Differential cross sections for $1s \rightarrow 1s$ capture in 293 keV proton-helium collisions calculated using the modified Faddeev approximation with normalized and unnormalized internuclear amplitudes and using an eikonally transformed electronic amplitude.

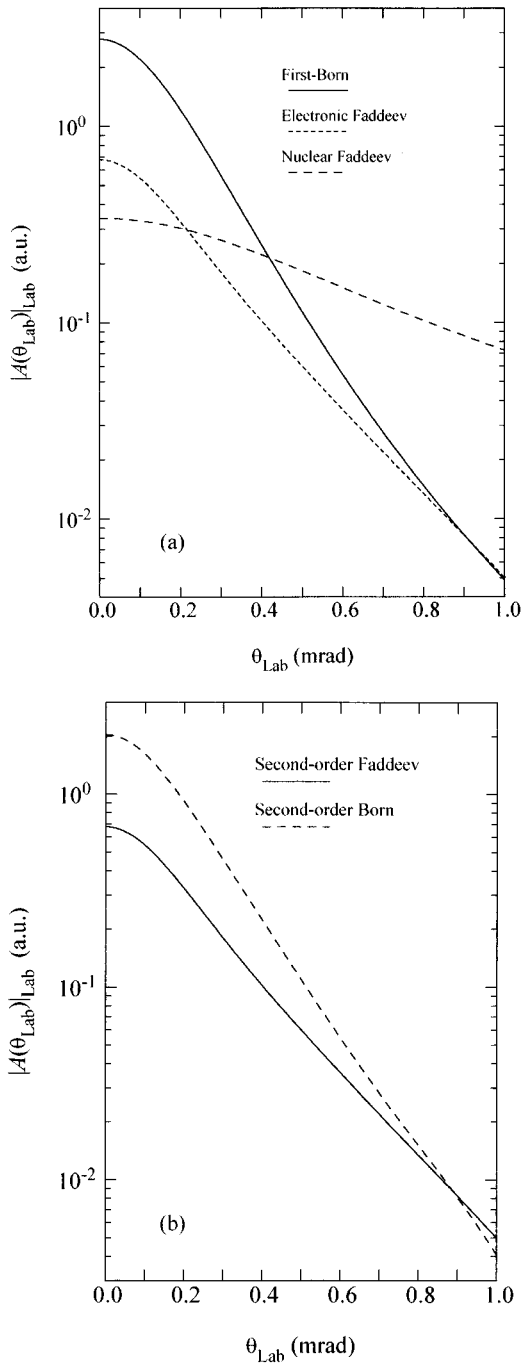


FIG. 7. Moduli of partial amplitudes of the full capture amplitude for (a) first Born, second-order electronic, and nuclear contributions and (b) second-order Born and modified Faddeev contributions.

less than 0.3 mrad, the effective-potential cross section is consistently 30% smaller, and at larger angles where the internuclear part dominates it is significantly in error. The behavior in these regions can be attributed to the decreased scattering allowed by the effective-potential amplitude, as was already pointed out in Fig. 3. Beyond 0.3 mrad, the enhancement arises because of decreased cancellation with the internuclear amplitude. The cross section obtained when the scattering states in the second-order term are not normalized according to Eqs. (51) and (52) is shown. This cross section is larger, some 30% at 0.0 mrad, even more beyond

0.4 mrad where, however, the effect is hardly noticeable relative to the contribution of the internuclear amplitude. Overall the larger cross section is a result of the second-order amplitude having a larger absolute magnitude.

Cross sections calculated using the F2 formalism with unmodified internuclear amplitude [Eq. (41)] and with the same internuclear contribution normalized to the eikonally transformed electronic amplitude [i.e., Eq. (33) transformed according to Eqs. (44) and (45)] are all shown in Fig. 6. All curves exhibit a $K^{-4}$ (or $J^{-4}$) momentum dependence beyond 0.6 mrad, which is consistent with the Coulomb scattering of the projectile off the target nucleus and with Eq. (41). Since $A_e$ exhibits a $K^{-6}$ dependence at the larger angles, so that its contribution can be neglected, it follows that the total cross section factors into the product of electronic and nuclear parts. It is to be noted that in proton-helium collisions at MeV energies the F2 cross sections agree very well with the experimental data in the region beyond 0.6 mrad (the Thomas peak region).

Figure 7(a) compares the moduli of the first Born amplitude $A_{B1}$, the normalized second-order Faddeev partial amplitude $A_e^{(2)}$ [Eq. (33)], and the internuclear partial amplitude $A_n$ [Eq. (41)]. Below 0.4 mrad, the first Born contribution is seen to be from two to four times larger than that of the normalized second-order partial amplitude. Significantly, it is seen that the moduli of the first Born and internuclear contributions become equal just beyond 0.4 mrad, precisely the angle where the modified Faddeev cross section and experimental data radically change slope (see Fig. 4). Otherwise, the internuclear modulus is comparatively very small, being a factor of 8 smaller at 0 mrad. That is, the electronic part of the amplitude dominates in the inner region and the internuclear part of the amplitude dominates in the outer region with little interaction between them.

In Fig. 7(b), the modulus of the second-order Faddeev partial amplitude [Eq. (33)] is compared with the corresponding second-order Born partial amplitude, which is obtained by setting the Sommerfeld parameters [defined in Eq. (34)] equal to zero in the Faddeev calculation. It is seen that a proper treatment of the two-body scattering significantly reduces the chance of capture by this mechanism. The unrealistically large second-order Born contribution at lower energies is a well-known feature of this approximation.

In summary, it has been shown that a modified second-order Faddeev approximation to the transition operator for electron capture at forward angles with a normalized internuclear contribution leads to a differential cross section in good agreement with experimental data for proton-helium collisions at lower energy. An explanation has been given for how the contribution of the internuclear potential arises and fits within a time-independent scattering formalism. Finally, a direct and explicit relation of the F2 theory to the second Born theory has been derived: A simple picture of capture involving the interaction of separate scatterings is maintained while a much more accurate treatment of each of the scatterings is employed.

## ACKNOWLEDGMENTS

I thank J. Macek for his hospitality while on sabbatical when part of this work was performed. This research is supported by the U.S. Department of Energy, Office of Energy Research, Office of Basic Energy Sciences, Division of Chemical Sciences. Calculations were performed on the Lawrence Livermore National Laboratory's CRAY-2 and the Pennsylvania State University's IBM 3090-600S computers.

[1] S. Alston, Phys. Rev. A **42**, 331 (1990); K. Taulbjerg and J. S. Briggs, J. Phys. B **16**, 3811 (1983).

[2] E. Horsdal-Pedersen, C. L. Cocke, and M. Stockli, Phys. Rev. Lett. **50**, 1910 (1983); H. Vogt, R. Schuch, E. Justiniano, M. Schulz, and W. Schwab, *ibid*. **57**, 2256 (1986).

[3] L. H. Thomas, Proc. R. Soc. London Ser. A **114**, 561 (1927); R. Shakeshaft and L. Spruch, Rev. Mod. Phys. **51**, 369 (1979); R. M. Drisko, Ph.D. thesis, Carnegie Institute of Technology, 1955 (unpublished).

[4] L. D. Faddeev, Zh. Éksp. Teor. Fiz. **39**, 1459 (1960) [Sov. Phys. JETP **12**, 1014 (1961)]; K. M. Watson, Phys. Rev. **88**, 1163 (1952); C. Lovelace, *ibid.* **135**, B1225 (1964).

[5] T. R. Bratton, C. L. Cocke, and J. R. Macdonald, J. Phys. B **10**, L517 (1977).

[6] E. Clementi and C. Roetti, At. Data Nucl. Data Tables **14**, 3707 (1981).

[7] C. J. Joachain, *Quantum Collision Theory* (North-Holland, Amsterdam, 1975), Chap. 19; M. L. Goldberger and K. M. Watson, *Collision Theory* (Wiley, New York, 1964).

[8] H. Marxer and J. S. Briggs, J. Phys. B **25**, 3823 (1992).

[9] R. McCarroll and A. Salin, J. Phys. B **1**, 163 (1968); J. S. Briggs, P. T. Greenland, and L. Kocbach, *ibid.* **15**, 3085 (1982).

[10] C. D. Lin and S. C. Soong, Phys. Rev. A **18**, 499 (1978).

[11] R. D. Rivarola, R. D. Piacentini, A. Salin, and Dž. Belkić, J. Phys. B **13**, 2601 (1980).

[12] S. Alston, Phys. Rev. A **38**, 636 (1988); H. Marxer, S. Alston, and J. Briggs, Z. Phys. D **5**, 35 (1987), and references therein.

[13] The coordinates transform as

$$\mathbf{r}_T=\beta\mathbf{r}_P+\mathbf{R}_P=\mathbf{r}+(1-\gamma)\mathbf{R},$$
$$\mathbf{R}_T=-(1-\alpha\beta)\mathbf{r}_P+\alpha\mathbf{R}_P=(1-\alpha)\mathbf{r}+[1-(1-\gamma)(1-\alpha)]\mathbf{R},$$
$$\mathbf{r}_P=\alpha\mathbf{r}_T-\mathbf{R}_T=\mathbf{r}-\gamma\mathbf{R},$$
$$\mathbf{R}_P=(1-\alpha\beta)\mathbf{r}_T+\beta\mathbf{R}_T=(1-\beta)\mathbf{r}+[1-\gamma(1-\beta)]\mathbf{R}.$$

[14] See S. Alston, Phys. Rev. A **38**, 6092 (1988); K. Dettmann and G. Leibfried, Z. Phys. **218**, 1 (1969).

[15] J. R. Oppenheimer, Phys. Rev. **31**, 349 (1928); H. C. Brinkman and H. A. Kramers, Proc. Acad. Sci. Amsterdam **33**, 973 (1930).

[16] J. C. Y. Chen and A. C. Chen, Adv. At. Mol. Phys. **8**, 71 (1972).

[17] S. T. Manson, Phys. Rev. **182**, 97 (1969).

[18] F. Herman and S. Skillman, *Atomic Structure Calculations* (Prentice-Hall, Englewood Cliffs, N.J., 1963).

[19] G. E. Forsythe, M. A. Malcolm, and C. B. Moler, *Computer Methods for Mathematical Computations* (Prentice-Hall, Englewood Cliffs, NJ, 1977), Chap. 5.

[20] S. R. Rogers and J. H. McGuire, J. Phys. B **10**, L497 (1977).